

Supplement of Atmos. Chem. Phys., 18, 9861–9877, 2018
<https://doi.org/10.5194/acp-18-9861-2018-supplement>
© Author(s) 2018. This work is distributed under
the Creative Commons Attribution 4.0 License.



Supplement of

Impacts of compound extreme weather events on ozone in the present and future

Junxi Zhang et al.

Correspondence to: Yang Gao (yanggao@ouc.edu.cn) and L. Ruby Leung (ruby.leung@pnnl.gov)

The copyright of individual parts of the supplement might differ from the CC BY 4.0 License.

Supplement

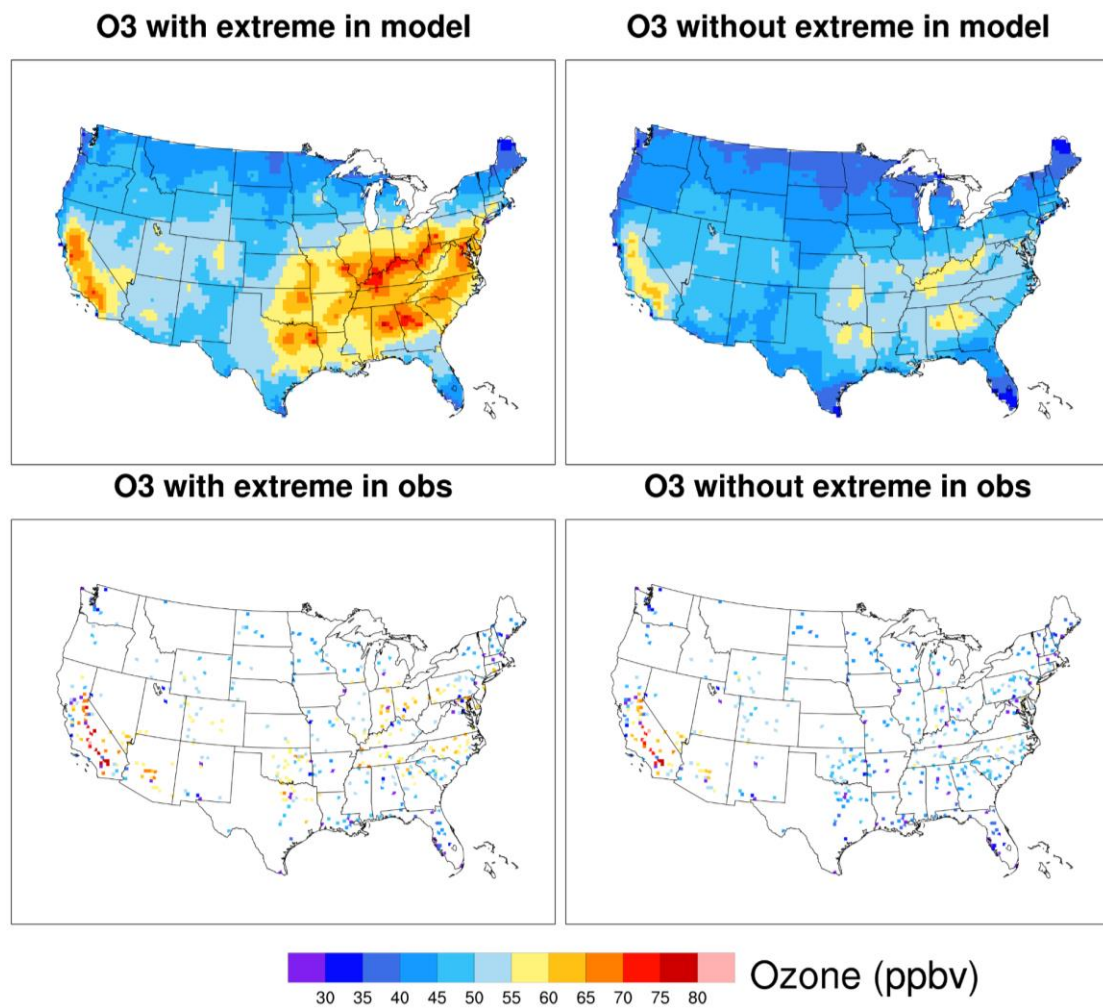


Fig. S1. Spatial distribution of summer ozone concentration with/without extreme events (heat wave, atmospheric stagnation and compound events) in model (WRF/Chem) and observations (NARR/AQS) during 2001-2010.

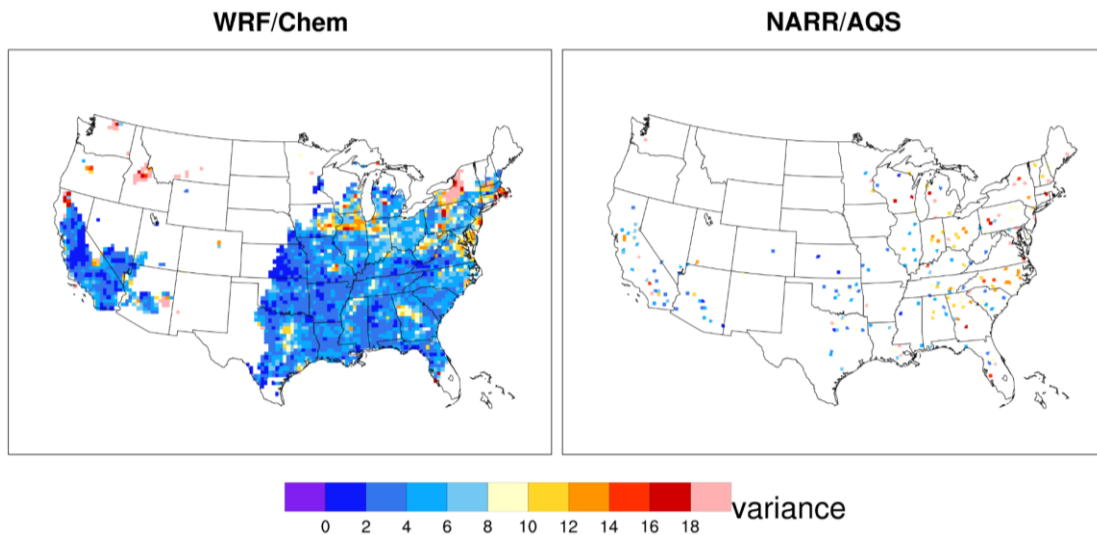


Fig. S2. Spatial distribution of variance of annual mean high ozone in each grid over the US for WRF/Chem simulations and observations from NARR/AQS during 2001-2010. Only grids having five years or more annual mean high ozone values are calculated.

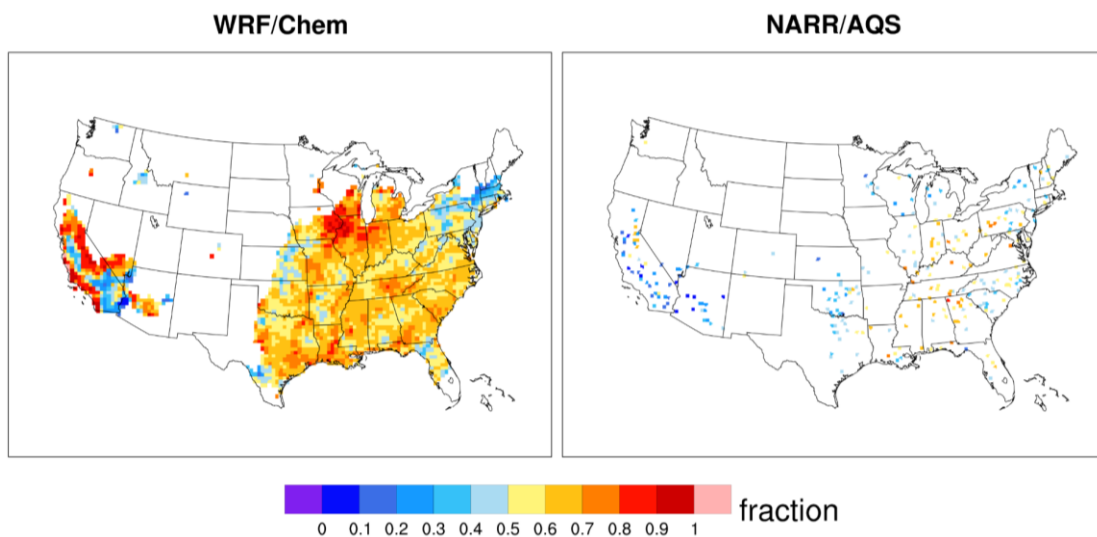


Fig. S3. Spatial distribution of the fraction of high ozone episodes that are driven by extreme events (heat wave, atmospheric stagnation and compound event) in model and observation during 2001-2010. Only grids having 10 days or more with high ozone are calculated. Blank areas in the model distribution (left figure) correspond to areas with no occurrence or few occurrence of high ozone episode.

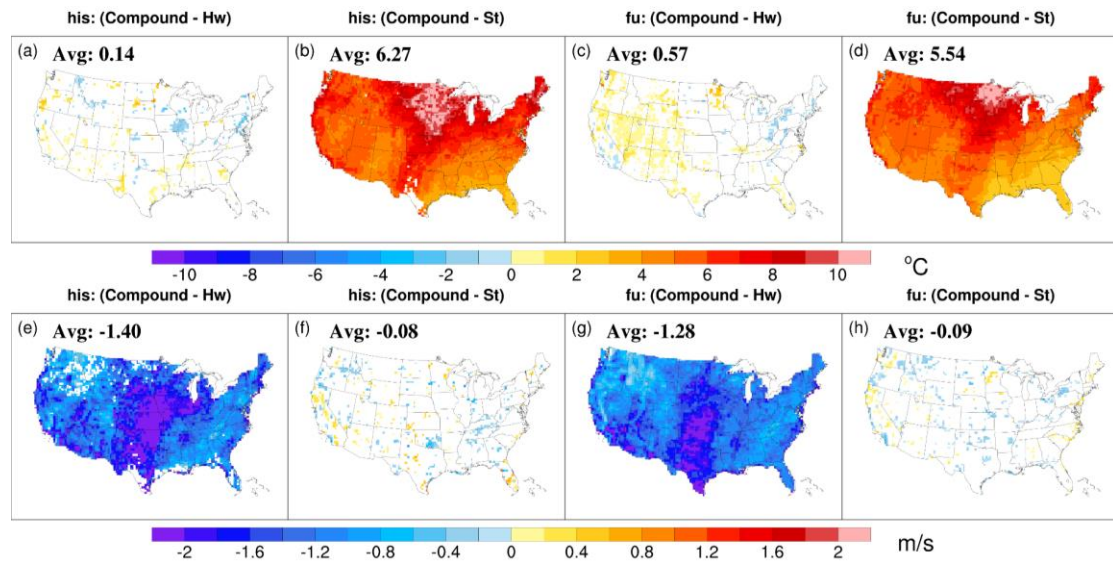


Fig. S4. Spatial distribution of the difference between compound event and single event in historical period and future period for daily maximum temperature at 2-m (top row) and wind speed at 10-m (bottom row) from WRF/Chem simulations. Only values with statistically significant differences (t-test: $\alpha=0.05$) between the compound event and single event are shown, and the mean differences are labeled on the top left.

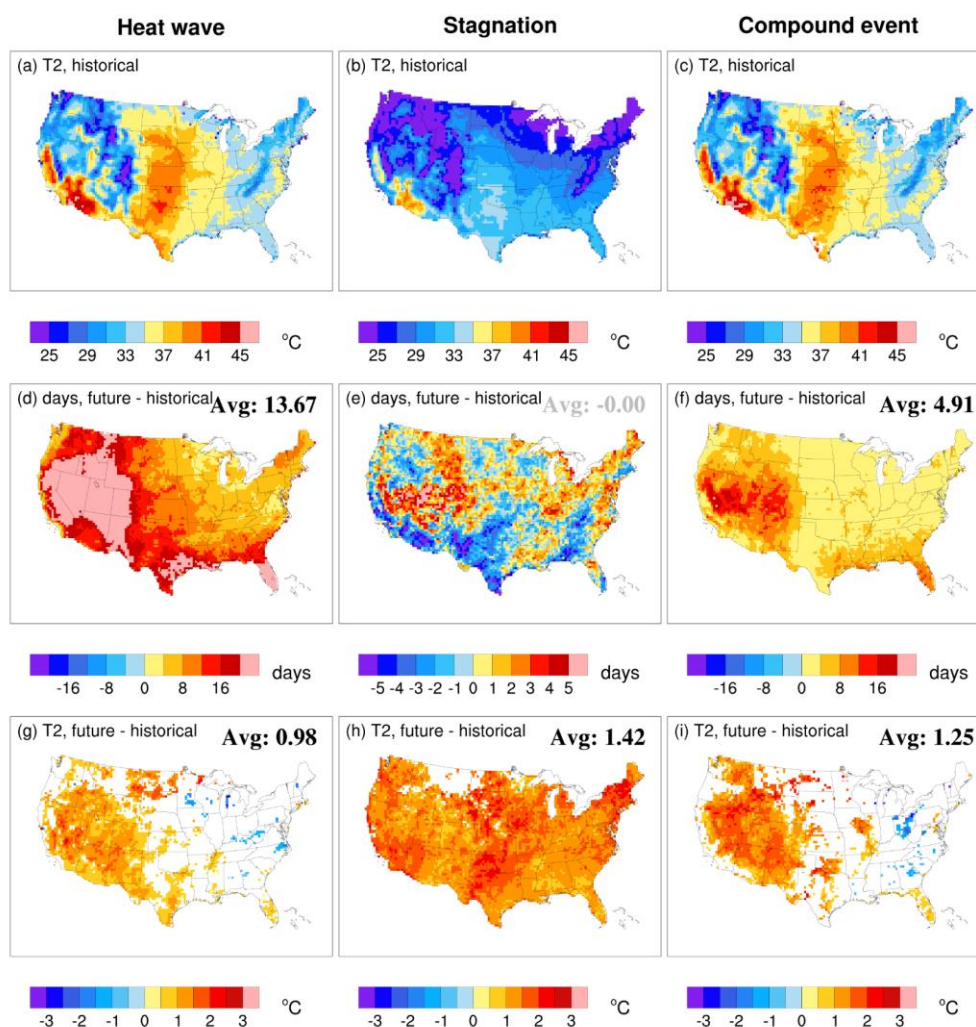


Fig. S5. Spatial distribution of daily maximum temperature at 2m during each type of extreme weather events in the historical period (top row) and the difference between future and present (bottom row) from WRF/Chem simulations. The middle row shows the change in the occurrence of each type of extreme events between future and present. In (d,e,f), a t-test ($\alpha=0.05$) is performed for the occurrence averaged over the US and values that are statistically significant are shown in black. In (g,h,i), only values with statistically significant differences (t-test: $\alpha=0.05$) between the future and historical periods are shown, and the mean differences are labeled on the top right.

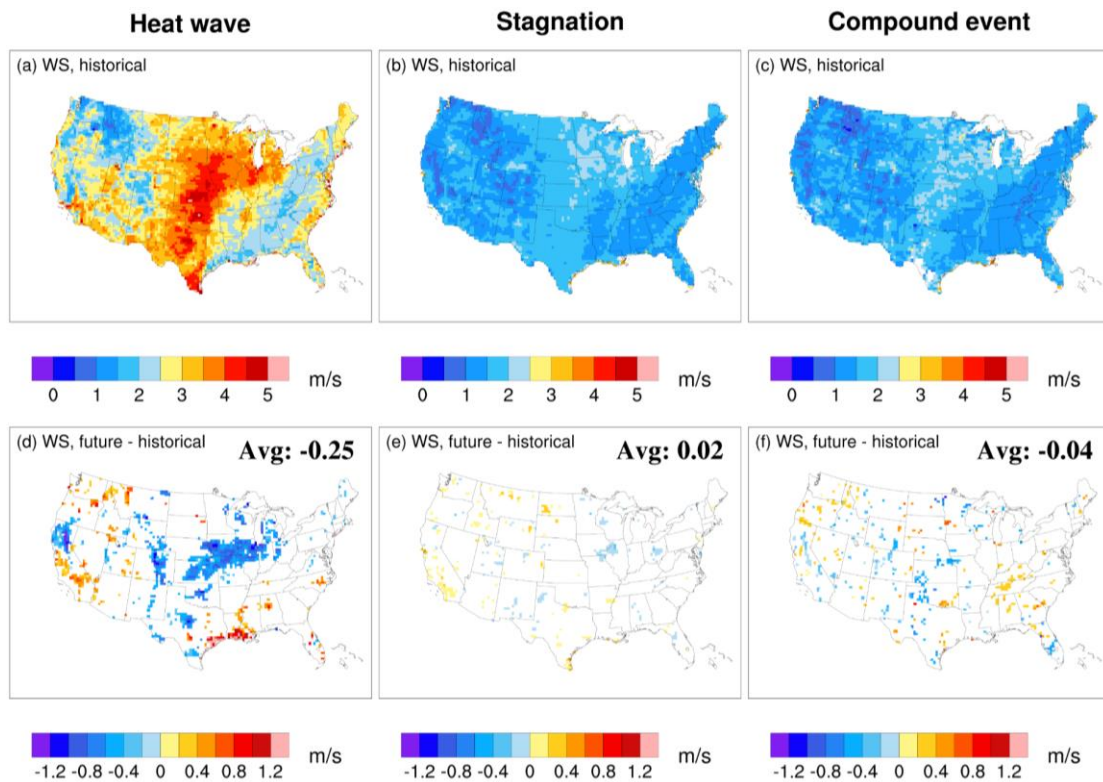


Fig. S6. Spatial distribution of 10-m wind speed (WS) during each type of extreme weather events in historical period (top row) and their future change (bottom row) from WRF/Chem simulations. In (d,e,f), only values with statistically significant differences (t-test: $\alpha=0.05$) between the future and historical periods are shown, and the mean differences are labeled on the top right.

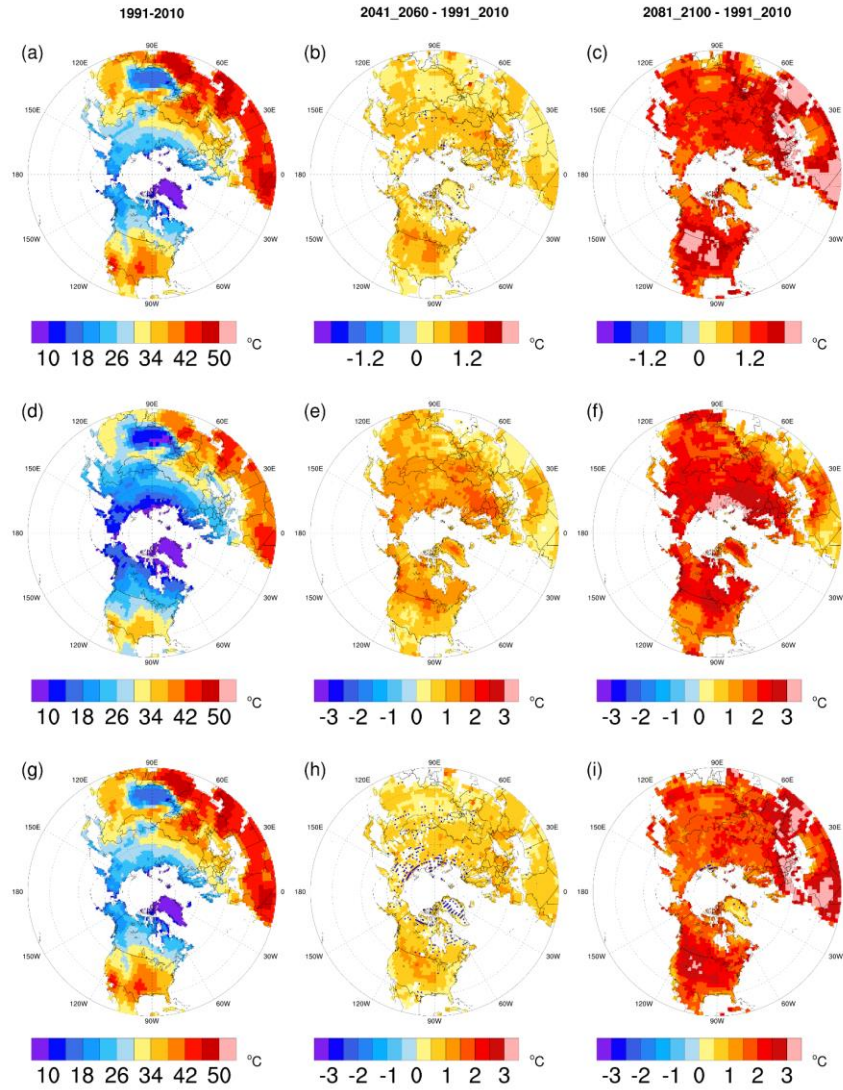


Fig. S7. Spatial distribution of historical (left column) and future changes in the mid-century (second column) and end-of-century (third column) in mean daily maximum 2-m temperature for heat waves (top row), atmospheric stagnation (middle row) and compound events (bottom row) from CMIP5 over land in the northern hemisphere north of 20° N. For the future changes, only grids showing model agreement are shown, with blue dots representing values with no statistical significance.

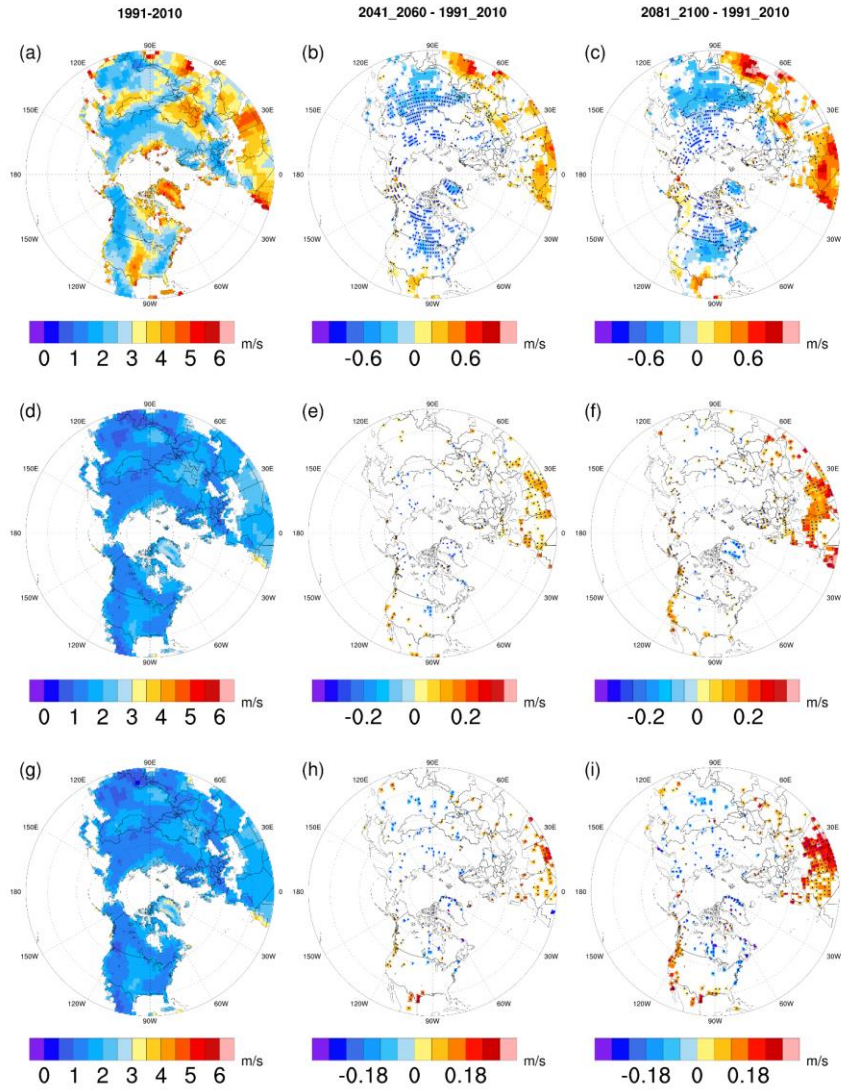


Fig. S8. Spatial distribution of historical (left column) and future changes in the mid-century (second column) and end-of-century (third column) in the mean 10-m wind speed for heat waves (top row), atmospheric stagnation (middle row) and compound events (bottom row) from CMIP5 over land in the northern hemisphere north of 20° N. For the future changes, only grids showing model agreement are shown, with blue dots representing values with no statistical significance.